

Superconducting properties of nanocrystalline MgB₂ thin films made by an *in situ* annealing process

X. H. Zeng, A. Sukiasyan, X. X. Xi,^{a)} Y. F. Hu, E. Wertz,
and Qi Li

Department of Physics, The Pennsylvania State University, University Park, Pennsylvania 16802

W. Tian, H. P. Sun, and X. Q. Pan

Department of Materials Science and Engineering, The University of Michigan, Ann Arbor, Michigan 48109

J. Lettieri, D. G. Schlom, C. O. Brubaker, and Zi-Kui Liu

Department of Materials Science and Engineering, The Pennsylvania State University, University Park, Pennsylvania 16802

Qiang Li

Division of Materials and Chemical Science, Brookhaven National Laboratory, Upton, New York 11973

(Received 4 May 2001; accepted for publication 20 July 2001)

We have studied the structural and superconducting properties of MgB₂ thin films made by pulsed-laser deposition followed by *in situ* annealing. The cross-sectional transmission electron microscopy reveals a nanocrystalline mixture of textured MgO and MgB₂ with very small grain sizes. A zero-resistance transition temperature (T_{c0}) of 34 K and a zero-field critical current density (J_c) of 1.3×10^6 A/cm² were obtained. The irreversibility field was ~ 8 T at low temperatures, although severe pinning instability was observed. The result is a step towards making the *in situ* deposition process a viable technique for MgB₂ Josephson junction technologies. © 2001 American Institute of Physics. [DOI: 10.1063/1.1405431]

Besides its potential for high-current and high-field applications, the superconductor MgB₂ (Refs. 1 and 2) has also stimulated great interest in its applications in microelectronics. It has been shown that MgB₂ is a phonon-mediated BCS superconductor³ with an energy gap of 5.2 meV at 4.2 K (Ref. 4) and a coherence length of 50 Å.⁵ Its grain boundaries do not have large detrimental effects on superconducting current transport.^{6,7} These properties promise that Josephson junctions of MgB₂ may be much easier to fabricate than those made from the high-temperature superconductors. Such junctions could have the performance of conventional superconductor junctions, such as Nb and NbN, but operate at a much higher temperature.

A MgB₂ film processing technique compatible with multilayer depositions is needed for Josephson junction applications. Currently, two main types of deposition processes have been used. The first type employs *ex situ* annealing of low-temperature deposited B or Mg+B films at 900 °C in Mg vapor. The resultant films exhibit bulk-like $T_{c0} \sim 39$ K (Refs. 8–10) and extremely high critical current density ($\sim 10^7$ A/cm² at low temperatures).^{11,12} However, the high-temperature *ex situ* annealing is unlikely to be compatible with multilayer device fabrications. The second type uses an *in situ* two-step process. Thin films or multilayers of Mg+B or Mg+MgB₂ are deposited at low temperatures, and then annealed *in situ* in the deposition chamber at about 600 °C.^{8,13–15} Although this process is potentially more compatible with junction fabrications, the early reports from various groups on *in situ* MgB₂ thin films show lower T_{c0} around or below 25 K.^{8,13–15} In this letter, we report that high

T_{c0} and J_c can be obtained in thin films made by an *in situ* process using pulsed-laser deposition (PLD) from a single target. The structural and superconducting properties of these films as compared to the *ex situ* annealed films and polycrystalline bulk samples are discussed.

The MgB₂ films were deposited on (0001)Al₂O₃ substrates by PLD with an *in situ* annealing procedure similar to those described by Blank *et al.*,¹³ Christen *et al.*,¹⁴ and Shinde *et al.*⁸ The PLD targets were prepared by pressing Mg powder with B or MgB₂ powder at room temperature. Some targets were wrapped in Nb foil and sintered at 600 °C for 30 min under a mixed gas of 95% Ar 5% H₂. Although both targets yielded comparable films, the results reported in this letter were from an unsintered target with a Mg:MgB₂ molar ratio of 4:1. The films were deposited at 250–300 °C in an Ar atmosphere (99.999% gas purity) of 120 mTorr. The Ar pressure was determined in the same way as described by Blank *et al.*,¹³ Christen *et al.*,¹⁴ and Grassano *et al.*:¹⁵ it generates a plume of the bluest color, which is characteristic of Mg. The plume at Ar pressures higher or lower than 120 mTorr is more greenish, which is characteristic of MgO. The background vacuum was in the low- to mid- 10^{-7} Torr range. The energy density of the laser beam was 5 J/cm² and the repetition rate was 5 Hz. The deposited films were then heated at a rate of 40 °C/min to 630 °C and held there for 10 min. The atmosphere during the heating and annealing was the same as during the deposition. After the *in situ* annealing, the films were cooled to room temperature in ~ 20 Torr Ar. The structures of the films were studied by both x-ray diffraction and cross-sectional transmission electron microscopy (TEM). TEM studies were performed in a JEOL 4000

^{a)}Electronic mail: xxx4@psu.edu

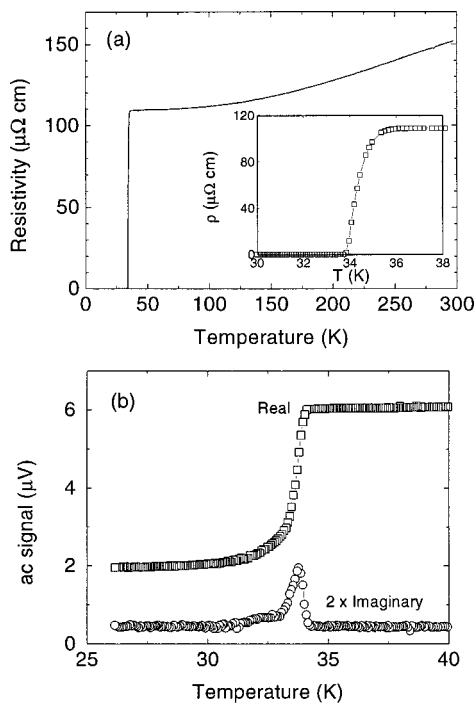


FIG. 1. (a) Resistivity vs temperature curve for a 4000-Å-thick MgB₂ film. (b) The ac susceptibility of the same film.

EX microscope operated at 400 kV, providing a point-to-point resolution of 0.17 nm.

The film deposited at 250–300 °C was likely a mixture of Mg and amorphous MgB₂ or B. Several processes are involved in the *in situ* annealing: Mg evaporation; MgB₂ phase formation, which is determined by the thermodynamics¹⁶ and forward kinetics;¹⁷ nucleation and growth of crystallites; and MgB₂ decomposition, which is determined by the thermodynamics¹⁶ and a kinetic barrier.¹⁷ In this annealing step, the film thickness changed from ~8000 to ~4000 Å, indicating the evaporation of excess Mg and possible decomposition of MgB₂. High-quality films are constrained by the balance of these processes, and a careful adjustment of the heating and annealing parameters such as temperature and duration is necessary. Once the conditions were properly controlled, we reproducibly prepared MgB₂ films with T_c of around 32 K (in over two dozen samples), and in two samples the zero-resistance temperature is as high as 34 K.

In Fig. 1(a) we plot the resistivity versus temperature curve for a 4000-Å-thick MgB₂ film. It shows a metallic behavior with a residual resistance ratio, $RRR = R(300\text{ K})/R(40\text{ K})$, of 1.4 and the resistivity at room temperature is $\sim 150\ \mu\Omega\text{ cm}$. Compared to high-density bulk samples, where $RRR = 25.3$ and $\rho(300\text{ K}) = 9.6\ \mu\Omega\text{ cm}$,¹⁸ the residual resistance ratio of the MgB₂ film is much smaller and the resistivity much higher. This is likely due to the small grain sizes and existence of MgO in the film, which will be discussed later, since precipitates of MgO at the grain boundaries will act as series-connected resistors to the MgB₂ grains. The superconducting transition temperature of the film, on the other hand, is close to that of bulk MgB₂. The zero-resistance temperature of the film is 34 K, which is shown more clearly in the inset of Fig. 1(a). The superconducting transition is further characterized by the ac suscepti-

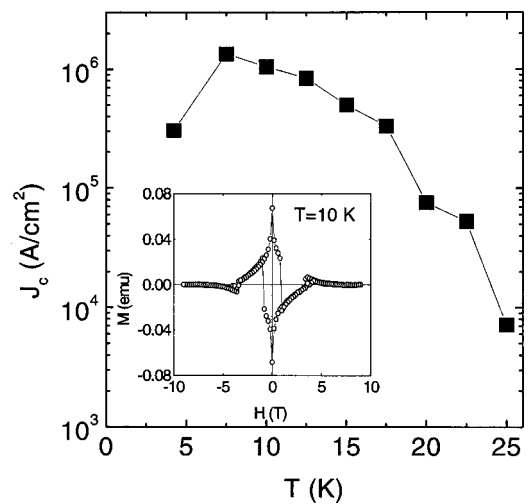


FIG. 2. Temperature dependence of the zero-field J_c of a 4000-Å-thick MgB₂ film. The inset shows the $M-H$ loop at $T = 10\text{ K}$.

bility, the result of which is shown in Fig. 1(b). The transition is relatively sharp with a full width at the half maximum of the imaginary-part signal being $\sim 0.8\text{ K}$, which is comparable to that found in the bulk.¹⁸

The critical current densities of the MgB₂ films were determined using the standard Bean model¹⁹ from dc magnetization curves measured with a Quantum Design PPMS magnetometer. In Fig. 2, the temperature dependence of J_c is plotted for a 4000-Å-thick MgB₂ film. A zero-field $J_c \sim 1.34 \times 10^6\text{ A/cm}^2$ was obtained at 7.5 K. The $M-H$ loop at 10 K for magnetic field $\mathbf{H} \perp$ film surface, which is 5 mm \times 4 mm in size, is shown in the inset. It shows a severe instability in flux pinning, or flux jump, which causes the collapse of circulating critical current so that the magnetization curve returns to the reversible magnetization branch (in the II and IV quadrants). The pinning instability is absent when $\mathbf{H} \parallel$ film surface, but the small film thickness yields erroneously large J_c values from the critical-state model. The actual closing of the hysteresis curve excluding the flux jump occurs at a field of $\sim 8\text{ T}$ at low temperatures, suggesting an irreversibility field similar to that found in bulk MgB₂.⁶

In contrast to *ex situ* annealed MgB₂ films, x-ray diffraction scans of our *in situ* annealed films revealed no discernable film peaks, indicating that the grain size was appreciably smaller. This is corroborated by the TEM results. Two MgB₂ films of different T_c , 22 and 32 K, respectively, were investigated. The result for the higher T_c sample is shown in Fig. 3. The dark-field image in Fig. 3(a) shows that the film consists of two layers with different contrasts. Figure 3(b) is a selected-area electron diffraction pattern taken from region I near the film/substrate interface. By measuring the position and intensity distribution of the diffraction rings, it is determined that they all belong to the rocksalt MgO phase. The MgO crystallites are very small and textured. Figure 3(c) is a diffraction pattern taken from region II close to the film surface using the same size selected-area aperture as for Fig. 3(b). In addition to the diffraction rings corresponding to the MgO phase, it also shows diffraction spots corresponding to the hexagonal MgB₂ phase. The diffraction spots indicated by the circles are due to the (001) planes, while those by the arrow heads arise from diffraction by the (110) planes of

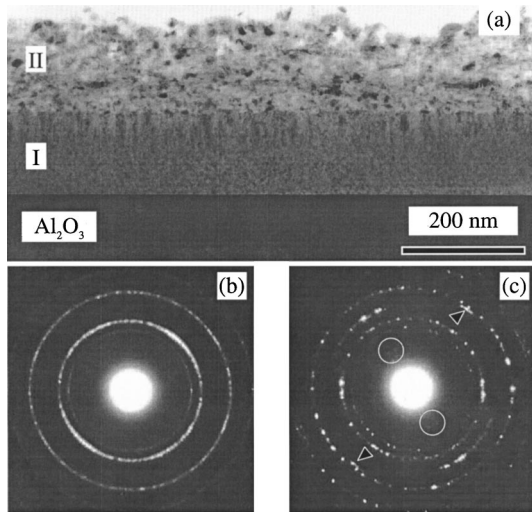


FIG. 3. (a) Dark-field TEM image showing a cross-sectional view of MgB₂ thin films. Selected-area electron diffraction patterns from (b) region I and (c) region II.

MgB₂. The (021) MgB₂ reflections are also detected. The discrete spots appear in Fig. 3(c) instead of nearly continuous rings in Fig. 3(b), indicating a larger grain size in region II. In both regions, the result indicates substantial oxygen contamination in the film. The MgB₂ grain size in region I must be less than about 5 nm to account for the absence of MgB₂ rings or spots in Fig. 3(b). In the film with lower T_c , region I is thinner than in the higher T_c films, and the MgB₂ diffraction patterns were not observed in both regions I and II. Additional details on the microstructural analysis will be published elsewhere.

The mechanism for the growth of the microstructure shown in Fig. 3 is not clear. Work is underway to better characterize each region by milling away the top region and measuring the properties of the remaining film. However, two features emerge from the above results. First, the T_{c0} value may correlate to the grain size. In the film with $T_c = 32$ K, the MgB₂ grains in region II are barely large enough so that their weak diffraction patterns can be observed. In the film with $T_c = 22$ K, the absence of the MgB₂ patterns indicates smaller grain sizes less than about 5 nm. In comparison, the *ex situ* annealed films are textured^{8,9,11} and have a grain size of order 10 nm,¹¹ and T_c is 39 K in various reports. When the grain size is close to the coherence length of MgB₂, the superconducting properties will be affected. While the 900 °C annealing in the *ex situ* process provides enough thermal energy for crystallization and texturing, the lower temperature during the *in situ* annealing limits the extent of these processes. The reason that the T_c value reported here is much higher than those in the early reports of *in situ* MgB₂ thin films^{8,13–15} may be that the grain size in our film is larger due to the details of the processing conditions. Second, severe oxygen contamination exists in the films. A separate x-ray photoelectron spectroscopy measurement of two films with different T_c , 17 and 32 K, respectively, shows that there is no appreciable difference in the oxygen content between the two films, and the Mg:B:O atomic ratio is 1.0:1.1:1.2. The extent of the detrimental effects of oxygen

contamination is not well understood, and Eom *et al.* even suggest that it may help to enhance the flux pinning.¹¹

In conclusion, we have deposited MgB₂ thin films by pulsed-laser deposition using an *in situ* annealing process. The T_{c0} obtained is much higher than the previously reported *in situ* films and J_c is comparable to those of the polycrystalline bulk samples even though the grain size in the films is extremely small. Because this deposition process is more compatible with multilayer deposition, it is important to demonstrate that high T_{c0} and J_c can be obtained using this process. Our results are a step towards making the *in situ* annealing technique a viable candidate for MgB₂ Josephson junction technologies.

This work is supported in part by ONR under Grant No. N00014-00-1-0294 for one of the authors (X.X.X.), by the NSF under Grant Nos. DMR-9875405 and DMR-9871177 for one of the authors (X.O.P.), DMR-9876266 and DMR-9972973 for one of the authors (Q.L.), DMR-9983532 for one of the authors (Z.K.L.), and by DOE through Grant No. DE-FG02-97ER45638 for one of the authors (D.G.S.). The work at BNL for one of the authors (Q.L.) is supported by DOE, Office of BES, under contract No. DE-AC02-98CH10886.

- ¹J. Nagamatsu, N. Nakagawa, T. Muranaka, Y. Zenitani, and J. Akimitsu, *Nature* (London) **410**, 63 (2001).
- ²R. J. Cava, *Nature* (London) **410**, 23 (2001).
- ³S. L. Bud'ko, G. Lapertot, C. Petrovic, C. E. Cunningham, N. Anderson, and P. C. Canfield, *Phys. Rev. Lett.* **86**, 1877 (2001).
- ⁴G. Karapetrov, M. Iavarone, W. K. Kwok, G. W. Crabtree, and D. G. Hinks, *Phys. Rev. Lett.* **86**, 4374 (2001).
- ⁵D. K. Finnemore, J. E. Ostenson, S. L. Bud'ko, G. Lapertot, and P. C. Canfield, *Phys. Rev. Lett.* **86**, 2420 (2001).
- ⁶D. C. Larbalestier, L. D. Cooley, M. O. Rikel, A. A. Polyanskii, J. Jiang, S. Patnaik, X. Y. Cai, D. M. Feldmann, A. Gurevich, A. A. Squitieri, M. T. Naus, C. B. Eom *et al.*, *Nature* (London) **410**, 186 (2001).
- ⁷Y. Bugoslavsky, G. K. Perkins, X. Qi, L. F. Cohen, and A. D. Caplin, *Nature* (London) **410**, 563 (2001).
- ⁸S. R. Shinde, S. B. Ogale, R. L. Greene, T. Venkatesan, P. C. Canfield, S. Bud'ko, G. Lapertot, and C. Petrovic, *Appl. Phys. Lett.* **79**, 227 (2001).
- ⁹H. Y. Zhai, H. M. Christen, L. Zhang, M. Paranthaman, C. Cantoni, B. C. Sales, P. H. Fleming, D. K. Christen, and D. H. Lowndes, *cond-mat* (2001).
- ¹⁰W. N. Kang, H.-J. Kim, E.-M. Choi, C. U. Jung, and S.-I. Lee, *Science* **292**, 1521 (2001).
- ¹¹C. B. Eom, M. K. Lee, J. H. Choi, L. Belenky, X. Song, L. D. Cooley, M. T. Naus, S. Patnaik, J. Jiang, M. O. Rikel, A. A. Polyanskii, A. Gurevich *et al.*, *Nature* (London) **411**, 558 (2001).
- ¹²S. H. Moon, J. H. Yun, H. N. Lee, J. I. Kye, H. G. Kim, W. Chung, and B. Oh, *cond-mat/0104230* (2001).
- ¹³D. H. A. Blank, H. Hilgenkamp, A. Brinkman, D. Mijatovic, G. Rijnders, and H. Rogalla, *Appl. Phys. Lett.* **79**, 394 (2001).
- ¹⁴H. Christen, H. Zhai, C. Cantoni, M. Paranthaman, B. Sales, C. Rouleau, D. Norton, D. Christen, and D. Lowndes, *Physica C* **353**, 157 (2001).
- ¹⁵G. Grassano, W. Ramadan, V. Ferrando, E. Bellingeri, D. Marré, C. Ferdeghini, G. Grasso, M. Putti, A. S. Siri, P. Manfrinetti, A. Palenzona, and A. Chincarini, *cond-mat/0103572* (2001).
- ¹⁶Z. K. Liu, D. G. Schlom, Q. Li, and X. X. Xi, *Appl. Phys. Lett.* **78**, 3678 (2001).
- ¹⁷Z. Y. Fan, D. G. Hinks, N. Newman, and J. M. Rowell, *Appl. Phys. Lett.* **79**, 87 (2001).
- ¹⁸P. C. Canfield, D. K. Finnemore, S. L. Bud'ko, J. E. Ostenson, G. Lapertot, C. E. Cunningham, and C. Petrovic, *Phys. Rev. Lett.* **86**, 2423 (2001).
- ¹⁹E. M. Gyorgy, R. B. van Dover, K. A. Jackson, L. F. Schneeneyer, and J. V. Waszczak, *Appl. Phys. Lett.* **55**, 283 (1989).